LANCZOS ALGORITHM FOR ELECTRON TRANSFER RATES IN SOLVENTS WITH COMPLEX SPECTRAL DENSITIES

AKIRA OKADA, VLADIMIR CHERNYAK, AND SHAUL MUKAMEL

Department of Chemistry, University of Rochester, Rochester, NY 14627

CONTENTS

I. INTRODUCTION

Solvation effects play an important role in electron transfer (ET) processes. In the weak-coupling (nonadiabatic) limit, these effects are primarily static, and enter through the solvent reorganization energy λ, which affects the activation free energy. As the donor–acceptor coupling strength is increased, solvent dynamics enters explicitly into the picture, and in the strong-coupling (adiabatic) regime the rate is determined by some properly

Advances in Chemical Physics, Volume 106, Electron Transfer—From Isolated Molecules to Biomolecules, Part One, edited by Joshua Jortner and M. Bixon. Series Editors I. Prigogine and Stuart A. Rice.
ISBN 0-471-25292-1

averaged solvent time scale [1–4]. Standard theories of ET incorporate the solvent via a single collective coordinate. Zusman had developed a theory that interpolates between the adiabatic and the nonadiabatic limits for a solvent with a single dielectric relaxation time (a Debye solvent) using the Smoluchowski equation [2]. That work triggered extensive theoretical activity [5–7]. The theory was extended to solvents with an arbitrary spectral density, using a single solvation coordinate that satisfies a Smoluchowski equation with a time-dependent (non-Markovian) kernel [8]. A microscopic definition of the relevant average solvent time scale that dominates the adiabatic rate was then obtained.

Additional high-frequency intramolecular vibrations have been incorporated into Fermi's Golden Rule [9]. Sumi and Marcus took into account the combined effect of intramolecular vibrational and diffusive solvent orientational motions on the ET rate [10]. By eliminating the fast intramolecular vibrational motions, they calculated the rate. Their model was used to explain the fractional power dependence of the ET rate on viscosity [11], and was extended to include an additional high-frequency intramolecular mode and to calculate the rate, keeping the intramolecular vibrational coordinates [12]. Barbara et al. considered a model that included three nuclear degrees of freedom: a solvent mode with a frictional response, an intramolecular low-frequency (classical) mode, and a high-frequency (quantum-mechanical) intramolecular mode [13].

Solvent nuclear motions are characterized by a broad range of time scales. Recent femtosecond ET experiments have addressed the role of complex solvent and solute nuclear relaxation dynamics in ET processes [13–17]. Femtosecond techniques, including time-dependent Stokes shift measurements [18], photon echoes [19–23], optical Kerr [24–26], transient grating [27], and multidimensional Raman echoes [28,29] have yielded detailed information with regard to solvent spectral densities in the frequency range of 0–1000 cm^{-1}. In this chapter we develop a microscopic theory that incorporates relaxation dynamics and solvents with complex nuclear spectral densities of arbitrary form in the calculation of electron transfer rates. Our approach is based on identifying a set of solvation coordinates, denoted nuclear collective modes (NCM), which can be uniquely constructed to represent a given spectral density [30]. Unlike previous theories, which start by assuming a number of coordinates, in the present treatment the only input is the spectral density. The number of necessary NCM then follows from the complexity of the spectral density. Our approach involves three steps. In step (1) we divide the nuclear coordinates into primary nuclear coordinates that couple to electronic dynamics directly, and secondary nuclear coordinates that couple to the primary nuclear coordinates and act as a heat bath. The procedure developed in [30] describes the effects of

nuclear modes by a finite number of effective collective solvent modes whose evolution is described by the Fokker–Planck or Smoluchowski operators. These modes are determined by the bath spectral densities, which contain all the relevant information about nuclear motions. However, the resulting system of equations constitutes coupled Liouville equations for density-matrix wave packets, which is still too complicated for direct numerical solution. In step (2) we make use of the fact that the electronic-coherence relaxation (dephasing) time scales are typically much faster compared with the ET rates. This allows us to eliminate the electronic coherences in the equations of motion, resulting in a closed system of equations for electronic population wave packets that depend on the solvent coordinates. To obtain the ET rate by solving these equations, the kernel of the integral equation in the space of collective coordinates needs to be inverted. This is accomplished in step (3) using the Lanczos expansion for inverting a linear operator. This algorithm constructs a set of Lanczos collective modes (LCM), which give the dominant contribution to the desired observables. This method is particularly powerful when only a few modes are necessary. The procedure given by steps (1)–(3) yields ET rates using a collective description of complex spectral densities. A clear distinction needs to be made between the solvation and the Lanczos modes. The nuclear collective modes describe the solvent dynamics alone as given by its spectral density, whereas the Lanczos collective modes represent how these nuclear motions affect the particular observable of interest (in our case this is the dynamics of the charge-transfer system coupled to the solvent). The number and character of NCM and LCM is generally different.

In Section II we derive closed equations that describe the dynamics of charge transfers among many sites, including the coupling to complex nuclear relaxation dynamics represented by an arbitrary spectral density. In Section III we obtain a formal expression for the ET rates using these equations. In Section IV we apply this method to a two-state system, and develop the Lanczos algorithm. These results are applied in Section V to model solvents with two relaxation time scales. The single-mode, two-mode, and the complete multimode expression are compared. In Section VI we summarize our procedure and outline how it may be applied to calculate the evolution of nuclear wave packets, which in turn may be used for calculating the time- and frequency-resolved fluorescence as well as pump–probe spectra of charge-transfer systems.

II. MULTIMODE DESCRIPTION OF SOLVATION DYNAMICS

ET reactions depend on the coupled dynamics of electrons and nuclei. Since many nuclear degrees of freedom are involved, any tractable procedure

must be based on a reduced description of nuclear dynamics. The reduction scheme developed in this chapter is based on constructing a few collective solvent coordinates that reproduce a given nuclear spectral density [30].

We consider the dynamics of a single-electron hopping among several molecules. We denote the state describing the electron is on the nth molecule by $|n\rangle$ with energy E_n. The Hamiltonian is

$$\hat{H} = \sum_n E_n|n\rangle\langle n| + \sum_{mn} J_{mn}|m\rangle\langle n| + \sum_j \left(\frac{\hat{p}_j'''^2}{2m_j'''} + \frac{m_j''' \omega_j'''^2 \hat{q}_j'''^2}{2} \right) - \sum_m \hat{q}_m^{(c)}|m\rangle\langle m| \tag{2.1}$$

Here the first two terms represent the purely electronic dynamics, J_{mn} being the ET coupling matrix element. The third term represents the pure solvent, modeled as a continuous distribution of harmonic coordinates. $\hat{p}_j'''$ and $\hat{q}_j'''$ are the momenta and coordinate operators, and m_j''' and ω_j''' are the masses and the frequencies of the oscillators representing nuclear (solute and solvent) motions. The last term represents the coupling of the electron to the solvent. The coordinate $\hat{q}_m^{(c)}$ is defined as

$$\hat{q}_m^{(c)} \equiv \sum_j m_j''' \omega_j'''^2 d_{j,m}''' \hat{q}_j''' \tag{2.2}$$

and $d_{j,m}'''$ is the displacement of the jth oscillator induced by populating the mth electronic state. All nuclear properties that affect the electronic motion are contained in the matrix of spectral densities $C_{m,k}(\omega)$

$$C_{m,k}(\omega) \equiv \frac{1}{2} \int_{-\infty}^{\infty} dt \exp(i\omega t) \langle [\hat{q}_m^{(c)}(t), \hat{q}_k^{(c)}(0)] \rangle \tag{2.3}$$

where the time evolution of $\hat{q}_{mn}^{(c)}(t)$ is calculated using the free nuclear Hamiltonian [the third term in Eq. (2.1)].

To obtain a reduced description of electronic dynamics in terms of a few nuclear collective variables, we recast the Hamiltonian [Eq. (2.1)] in a different form, by introducing a set of N primary oscillators with momenta $\hat{p}_\alpha'$ and coordinates $\hat{q}_\alpha'$ ($\alpha = 1, 2, \ldots, N$), coupled to the electronic degrees of freedom and to a set of bath oscillators $\hat{p}_j''$ and $\hat{q}_j''$ [31–34]. The Hamiltonian

then becomes

$$\hat{H} = \sum_n E_n|n\rangle\langle n| + \sum_{mn} J_{mn}|m\rangle\langle n| + \sum_{\alpha=1}^{N}\left(\frac{\hat{p}_\alpha'^2}{2m_\alpha} + \frac{m_\alpha\omega_\alpha^2\hat{q}_\alpha'^2}{2}\right) - \sum_{\alpha m} m_\alpha\omega_\alpha^2 d'_{\alpha,m}\hat{q}'_\alpha|m\rangle\langle m| + \sum_{j\alpha}\left[\frac{\hat{p}_{j\alpha}''^2}{2m''_{j\alpha}} + \frac{m''_{j\alpha}\omega''^2_{j\alpha}}{2}\left(\hat{q}''_{j\alpha} - \frac{c_{j\alpha}}{m''_{j\alpha}\omega''^2_{j\alpha}}\hat{q}'_\alpha\right)^2\right] \tag{2.4}$$

Hereafter, we shall use the scaled variables p_α, q_α, and $d_{\alpha,m}$ instead of p'_α, q'_α, and $d'_{\alpha,m}$

$$p_\alpha \equiv \left(\frac{m_\alpha\omega_\alpha^2}{2}\right)^{-1/2} p'_\alpha; \qquad q_\alpha \equiv \left(\frac{m_\alpha\omega_\alpha^2}{2}\right)^{1/2} q'_\alpha; \qquad d_{\alpha,m} \equiv \left(\frac{m_\alpha\omega_\alpha^2}{2}\right)^{1/2} d'_{\alpha,m} \tag{2.5}$$

We further assume that the bath modes are fast compared with the primary modes, the temperature is high, and the primary oscillators are overdamped. The matrix of spectral densities can then be represented in the form

$$C_{mn}(\omega) = \sum_{\alpha=1}^{N} 2d_{\alpha,m}d_{\alpha,n}\frac{\Lambda_\alpha\omega}{\omega^2 + \Lambda_\alpha^2} \tag{2.6}$$

Here Λ_α is the relaxation rate of the primary mode α. In this model it is possible to eliminate the bath degrees of freedom as well as the momenta of the overdamped primary modes. We then obtain the equation of motion of the reduced density matrix $\hat{\rho}(\mathbf{q}, t)$

$$\frac{d\hat{\rho}(\mathbf{q},t)}{dt} = -i[\hat{H}_e, \hat{\rho}] + i\sum_{m\alpha} 2d_{\alpha,m}q_\alpha[|m\rangle\langle m|, \hat{\rho}] + \sum_{\alpha=1}^{N}\Lambda_\alpha\frac{\partial}{\partial q_\alpha}\left(q_\alpha + \frac{k_B T}{2}\frac{\partial}{\partial q_\alpha}\right)\hat{\rho} - \frac{1}{2}\sum_{m\alpha}\Lambda_\alpha d_{\alpha,m}\left[|m\rangle\langle m|, \frac{\partial\hat{\rho}}{\partial q_\alpha}\right]_+ \tag{2.7}$$

where $\rho(\mathbf{q}, t)$ is an operator in the electronic space, $[.,.]$ and $[.,.]_+$ denote an commutator and an anticommutator, respectively. $\mathbf{q}$ denotes the set of

collective coordinates q_α representing the effects of all nuclear degrees of freedom. Taking the electronic matrix elements

$$\rho_{mn}(\mathbf{q}, t) \equiv \langle m|\hat{\rho}(\mathbf{q}, t)|n\rangle \tag{2.8}$$

we find that the equation of motion includes electronic coherences $\rho_{mn}(\mathbf{q}, t)$ $(m \neq n)$ as well as populations $\rho_{mm}(\mathbf{q}, t)$. We assume that the coherence relaxation time scales are much shorter than those of the populations (the spectral-diffusion limit). Coherences may then be eliminated to obtain closed equations of motion for the electronic population wave packets $\rho_{mm}(\mathbf{q}, t)$ [30]

$$\frac{d\rho_{mm}(\mathbf{q}, t)}{dt} = \sum_{\alpha=1}^{N} \Lambda_\alpha \frac{\partial}{\partial q_\alpha}\left((q_\alpha - d_{\alpha,m}) + \frac{k_B T}{2}\frac{\partial}{\partial q_\alpha}\right)\rho_{mm}(\mathbf{q}, t) + \sum_{m'} K_{mm'}(\mathbf{q})\rho_{m'm'}(\mathbf{q}, t) \tag{2.9}$$

Here

$$K_{mm'}(\mathbf{q}) \equiv 2\pi|J_{mm'}|^2\,\delta[U_m(\mathbf{q}) - U_{m'}(\mathbf{q})], \qquad m \neq m' \tag{2.10}$$

$$K_{mm}(\mathbf{q}) \equiv -\sum_{m'(m'\neq m)} K_{m'm}(\mathbf{q}) \tag{2.11}$$

$$U_m(\mathbf{q}) \equiv \sum_{\alpha=1}^{N}[(q_\alpha - d_{\alpha,m})^2 - d_{\alpha,m}^2] + E_m \tag{2.12}$$

The reorganization energy of the collective coordinate α for the transition between the m' and m electronic states is denoted by $\lambda_{\alpha,mm'}$

$$\lambda_{\alpha,mm'} \equiv (d_{\alpha,m} - d_{\alpha,m'})^2 \tag{2.13}$$

and the total reorganization energy for the transition between the m' and m electronic states $\lambda_{mm'}$ is

$$\lambda_{mm'} \equiv \sum_{\alpha=1}^{N} \lambda_{\alpha,mm'} \tag{2.14}$$

The corresponding free-energy gap defined as the free energy of m minus that of m' is

$$\Delta G_{mm'}^{free} = -\sum_{\alpha=1}^{N} d_{\alpha,m}^2 + E_m + \sum_{\alpha=1}^{N} d_{\alpha,m'}^2 - E_{m'} \tag{2.15}$$

The potential difference $U_m(\mathbf{q}) - U_{m'}(\mathbf{q})$ constitutes a reaction (or solvation) coordinate for the transition between m' and m

$$x_{mm'}(\mathbf{q}) \equiv U_m(\mathbf{q}) - U_{m'}(\mathbf{q}) \tag{2.16}$$

Equation (2.10) implies that the transition between electronic states takes place only at nuclear configurations where the reaction coordinate vanishes [Eq. (2.10)]

$$U_m(\mathbf{q}) - U_{m'}(\mathbf{q}) = 0 \tag{2.17}$$

The $(N-1)$-dimensional curve-crossing manifold in the N-dimensional space of collective coordinates defined by Eq. (2.17) will be denoted $\mathcal{M}_{mm'}$. The remainder of this chapter focuses on an approximate solution of Eq. (2.9).

III. GREEN FUNCTION EXPRESSION FOR THE RATE MATRIX

We shall transform the equations of motion for the population wave packets [Eq. (2.9)], which depend on N collective coordinates q_α, into integral equations for wave packets in the $(N-1)$-dimensional space defined by the constraint [Eq. (2.20)]. We start by partitioning Eq. (2.9) in the form

$$\frac{d\rho(\mathbf{q},t)}{dt} = -iL^{(0)}\rho(\mathbf{q},t) - iL^{(1)}\rho(\mathbf{q},t) \tag{3.1}$$

where $\rho(\mathbf{q},t)$ is a vector whose mth component is a nuclear wave packet representing the population of the mth electronic state $\rho_{mm}(\mathbf{q},t)$. L_0 represents the first term and L_1 the second term in the RHS of Eq. (2.9). We next introduce the Green function $G_m(\mathbf{q},\mathbf{q}';t)$ of the Smoluchowski equations [Eq. (2.9) with $L^{(1)} = 0$], defined by

$$\exp(-iL^{(0)}_{mm}t)\rho'_{mm}(\mathbf{q},0) = \int d\mathbf{q}'\, G_m(\mathbf{q},\mathbf{q}';t)\rho'_{mm}(\mathbf{q}',0) \tag{3.2}$$

where

$$G_m(\mathbf{q},\mathbf{q}';t) \equiv \prod_\alpha G_{m\alpha}(q_\alpha, q'_\alpha; t) \tag{3.3}$$

$$G_{m\alpha}(q_\alpha, q'_\alpha; t) \equiv \frac{1}{\sqrt{2\pi\sigma_\alpha(t)}} \exp\left(-\frac{1}{2\sigma_\alpha(t)}\left[(q_\alpha - d_{\alpha,m}) - (q'_\alpha - d_{\alpha,m})M_\alpha(t)\right]^2\right), \quad (3.4)$$

$$\sigma_\alpha(t) \equiv \frac{k_b T}{2}\{1 - [M_\alpha(t)]^2\}, \qquad M_\alpha(t) \equiv \exp(-\Lambda_\alpha t) \quad (3.5)$$

Using this Green function we can recast the solution of Eq. (2.9) as

$$\rho_{mm}(\mathbf{q}, t) = \int d\mathbf{q}'\, G_m(\mathbf{q}, \mathbf{q}'; t)\rho_{mm}(\mathbf{q}', 0) - \sum_{m'} \int_0^t dt' \int d\mathbf{x}'_{mm'}\, 2\pi |J_{mm'}|^2 G_m(\mathbf{q}, \mathbf{x}'_{mm'}; t - t') r_{mm'}(\mathbf{x}'_{mm'}, t') \quad (3.6)$$

where we have introduced the differences between population wave packets

$$r_{mn}(\mathbf{x}_{mn}, t) \equiv \rho_{mm}(\mathbf{x}_{mn}, t) - \rho_{nn}(\mathbf{x}_{mn}, t) \quad (3.7)$$

and $\mathbf{x}_{mn}$ is a vector representing a point that belongs to the curve-crossing manifold $\mathcal{M}_{mn}$. The integral $\int d\mathbf{x}_{mm'} \cdots$ is defined as

$$\int d\mathbf{x}_{mm'} \cdots \equiv \int d\mathbf{q}\, \delta[U_m(\mathbf{q}) - U_{m'}(\mathbf{q})] \cdots \quad (3.8)$$

Using Eq. (3.6), we obtain the following closed integral equations for r_{mn}

$$r_{mn}(\mathbf{x}_{mn}, t) = S_{mn}(\mathbf{x}_{mn}, t) - \sum_{m'} \int_0^t dt' \int d\mathbf{x}'_{mm'}\, 2\pi |J_{mm'}|^2 G_m(\mathbf{x}_{mn}, \mathbf{x}'_{mm'}; t - t') r_{mm'}(\mathbf{x}'_{mm'}, t) + \sum_{n'} \int_0^t dt' \int d\mathbf{x}'_{nn'}\, 2\pi |J_{nn'}|^2 G_n(\mathbf{x}_{mn}, \mathbf{x}'_{nn'}; t - t') r_{nn'}(\mathbf{x}'_{nn'}, t') \quad (3.9)$$

where

$$S_{mn}(\mathbf{x}_{mn}, t) \equiv \int d\mathbf{q}'\, G_m(\mathbf{x}_{mn}, \mathbf{q}'; t)\rho_{mm}(\mathbf{q}', 0) - \int d\mathbf{q}'\, G_n(\mathbf{x}_{mn}, \mathbf{q}'; t)\rho_{nn}(\mathbf{q}', 0) \quad (3.10)$$

The population wave packets $\rho_{mm}(\mathbf{q}, t)$ are obtained by substituting the solution of Eq. (3.9), $r_{mn}(\mathbf{x}_{mn}, t)$ in the RHS of Eq. (3.6).

To define the ET rate we consider the population of the mth electronic state, $P_m(t)$

$$P_m(t) \equiv \int d\mathbf{q}\, \rho_{mm}(\mathbf{q}, t) \tag{3.11}$$

Integrating Eq. (3.6) over $\mathbf{q}$ yields

$$P_m(t) = P_m(0) - \sum_{m'} \int_0^t dt' \int d\mathbf{x}'_{mm'}\, 2\pi |J_{mm'}|^2 r_{mm'}(\mathbf{x}'_{mm'}, t') \tag{3.12}$$

The ET rate matrix $\mathbf{K}(t)$ is defined by the generalized master equation [35]

$$\frac{d}{dt} P(t) \equiv \int_0^t d\tau\, \mathbf{K}(t-\tau) P(\tau) \tag{3.13}$$

where $P(t)$ is a vector with elements

$$[P(t)]_m \equiv P_m(t) \tag{3.14}$$

and $\mathbf{K}(t)$ is a matrix with elements $K_{mm'}(t)$. $K_{mm'}$ for $m \neq m'$ is the ET rate from state m' to m. We shall express the rate matrix $\mathbf{K}(t)$ in terms of a set of the solutions of Eq. (3.9) obtained using different initial conditions. The lth initial condition is

$$[\rho(\mathbf{q}, 0)]_m = \delta_{ml} \bar{\rho}_{ll}^{(eq)}(\mathbf{q}) \tag{3.15}$$

where the equilibrium distribution for the lth electronic state is

$$\bar{\rho}_{ll}^{(eq)}(\mathbf{q}) \equiv \prod_{\alpha} \sqrt{\frac{1}{\pi k_B T}} \exp\left(-\frac{1}{k_B T} (q_\alpha - d_{\alpha,l})^2 \right) \tag{3.16}$$

We further denote $r_{mn}(\mathbf{x}_{mn}, t)$ and $P_m(t)$ obtained using the lth initial condition by $r_{mn;l}(\mathbf{x}_{mn}, t)$ and $P_{m;l}(t)$, respectively. We denote the Laplace transform of $F(t)$ by $F(s)$

$$F(s) \equiv \int_0^\infty dt\, e^{-st} F(t) \tag{3.17}$$

The formal solution of Eq. (3.13) is obtained using a Laplace transform

$$P(s) = [s\mathbf{1} - \mathbf{K}(s)]^{-1} P(t = 0) \tag{3.18}$$

Comparing Eq. (3.18) with the Laplace transform of Eq. (3.12) finally yields

$$\mathbf{K}(s) = s\mathbf{1} - \mathbf{T}(s)^{-1} \tag{3.19}$$

where

$$[\mathbf{T}(s)]_{ml} = \frac{1}{s}\left(\delta_{ml} - \sum_{m'} \int d\mathbf{x}'_{mm'}\, 2\pi |J_{mm'}|^2 r_{mm';l}(\mathbf{x}'_{mm'}, s)\right) \tag{3.20}$$

The rate matrix can thus be calculated by solving the integral equation (3.9) for $r_{mm';l}(\mathbf{x}'_{mm'}, s)$ using several initial conditions and substituting the solutions in Eqs. (3.19) and (3.20).

IV. LANCZOS EXPANSION OF THE RATE IN DOMINANT NUCLEAR MODES

In this section we calculate the ET rate by solving Eqs. (3.6) and (3.9) for a two-state donor–acceptor system. We shall omit the subscripts of J_{12}, $\mathbf{x}_{12}$, and r_{12} because only a single potential crossing manifold $\mathcal{M} \equiv \mathcal{M}_{12}$ appears in this case. We further focus on the zero-frequency rate $K_{21} \equiv K_{21}(s = 0)$. which appears in the ordinary master equation, when memory effects can be neglected.

We adopt the following operator notation: The action of an operator $\hat{h}$ on a function $r(\mathbf{x})$ on $\mathcal{M}$ is defined by

$$\hat{h}r(\mathbf{x}) = \int d\mathbf{x}'\, h(\mathbf{x}, \mathbf{x}')r(\mathbf{x}') \tag{4.1}$$

The product $\hat{h}\hat{g}$ of two operators $\hat{h}$ and $\hat{g}$ is similarly represented by

$$\hat{h}\hat{g}(\mathbf{x}, \mathbf{x}') = \int d\mathbf{x}''\, h(\mathbf{x}, \mathbf{x}'')g(\mathbf{x}'', \mathbf{x}') \tag{4.2}$$

the unit operator $\hat{I}$ on $\mathcal{M}$ is represented by the δ function: $I(\mathbf{x}, \mathbf{x}') = \delta(\mathbf{x} - \mathbf{x}')$ and $h^{-1}(\mathbf{x}, \mathbf{x}')$ represents the operator $\hat{h}^{-1}$ inverse to $\hat{h}$. In Appendix A we obtain the following expression for the ET rate using Eqs. (3.19) and (3.20) together with Eq. (3.9)

$$K_{21} = 2\pi |J|^2 \int d\mathbf{x}\, \hat{h}^{-1} \bar{\rho}_{11}^{(eq)}(\mathbf{x}) \tag{4.3}$$

where

$$h(\mathbf{x}, \mathbf{x}') \equiv \delta(\mathbf{x} - \mathbf{x}') + 2\pi|J|^2 g(\mathbf{x}, \mathbf{x}') \tag{4.4}$$

$$g(\mathbf{x}, \mathbf{x}') \equiv \int_0^\infty dt \sum_{m=1}^{2} [G_m(\mathbf{x}, \mathbf{x}', t) - \bar{\rho}_{mm}^{(eq)}(\mathbf{x})] \tag{4.5}$$

This expression gives the rate to all orders in the electronic coupling J. In the nonadiabatic ($J \to 0$) limit this gives

$$K_{NA} = 2\pi|J|^2 \int d\mathbf{x}\, \bar{\rho}_{11}^{(eq)}(\mathbf{x}) \tag{4.6}$$

and in the opposite, adiabatic ($J \to \infty$) limit we obtain

$$K_{AD} = \int d\mathbf{x}\, \hat{g}^{-1} \bar{\rho}_{11}^{(eq)}(\mathbf{x}) \tag{4.7}$$

In Appendix B we outline the Lanczos algorithm for inverting the kernel h [36,37]. The method is based on an assumption that the initial condition; that is, the wave packet $\rho_{11}^{(eq)}(\mathbf{x})$ in Eq. (4.3) can be expanded in a finite number of eigenmodes of h. We can develop a hierarchy of M-mode approximations for the rate $K_{21}^{(M)}$, and check for convergence by gradually increasing M. For sufficiently large M the inversion of the kernel is exact. The single-mode approximation assumes that all solvent variables, other than the reaction coordinate, equilibrate rapidly. Higher members of the hierarchy give improved approximations that hold to higher order in the electronic coupling J. In the lowest level ($M = 1$) we have

$$K_{21}^{(1)} = \frac{2\pi|J|^2 g_0}{1 + 2\pi|J|^2 g_1/g_0} \tag{4.8}$$

where

$$g_0 \equiv \int \mathrm{d}\mathbf{x}\, \bar{\rho}_{11}^{(eq)}(\mathbf{x}) \tag{4.9}$$

$$g_n \equiv \int d\mathbf{x}\, \hat{g}^n \bar{\rho}_{11}^{(eq)}(\mathbf{x}), \qquad \text{for } n \geq 1 \tag{4.10}$$

Using Eqs. (3.3)–(3.5), (3.16), (4.9), and (4.10) we obtain

$$g_0 = \frac{1}{\sqrt{4\pi\lambda k_B T}} \exp\left(-\frac{(\Delta G^0 + \lambda)^2}{4\lambda k_B T}\right) \tag{4.11}$$

$$g_1 = g_0^2 \tau \tag{4.12}$$

where

$$\tau = \int_0^\infty dt f_+(t) + \exp\left(\frac{\Delta G^0}{k_B T}\right) \int_0^\infty dt f_-(t) \tag{4.13}$$

$$\Delta G^0 \equiv \Delta G_{21}^{free} \tag{4.14}$$

$$\lambda \equiv \sum_{\alpha=1}^{N} \lambda_\alpha \tag{4.15}$$

$$f_\pm(t) = \frac{1}{\sqrt{1 - M(t)^2}} \exp\left(-\frac{(\Delta G^0 \pm \lambda)^2}{4\lambda k_B T} \frac{2M(t)}{1 + M(t)}\right) - 1 \tag{4.16}$$

Here $M(t)$ is a normalized autocorrelation function of the reaction coordinate

$$M(t) = \frac{\int d\mathbf{q} \int d\mathbf{q}' \sum_\alpha \lambda_\alpha q_\alpha G_1(\mathbf{q}, \mathbf{q}'; t) q'_\alpha \bar{\rho}_{11}^{(eq)}(\mathbf{q}')}{\int d\mathbf{q} \sum_\alpha \lambda_\alpha q_\alpha^2 \bar{\rho}_{11}^{(eq)}(\mathbf{q})} \tag{4.17}$$

Using Eqs. (3.3), (3.4), (3.16), and (4.17), we have

$$M(t) = \sum_\alpha \frac{\lambda_\alpha}{\lambda} e^{-\Lambda_\alpha t} \tag{4.18}$$

where lower subscripts indicating electronic states were omitted

$$(\lambda \equiv \lambda_{12}, \lambda_\alpha \equiv \lambda_{\alpha,12}).$$

Equation (4.8) may be recast in the form

$$K_{21}^{(1)} = \frac{K_{NA}}{1 + K_{NA}\tau} \tag{4.19}$$

Using Eqs. (4.6) and (4.11), we recover the Marcus expression of the nonadiabatic rate

$$K_{NA} = \frac{2\pi J^2}{\hbar} \frac{1}{\sqrt{4\pi\lambda k_B T}} \exp\left(-\frac{(\Delta G^0 + \lambda)^2}{4\lambda k_B T} \right) \tag{4.20}$$

Equation (4.19) interpolates between the nonadiabatic ($J \to 0$) and adiabatic limits ($J \to \infty$) where it attains the value τ^{-1}. τ is an averaged solvent time scale given by Eq. (4.13). Equation (4.8) coincides with the earlier result derived using projection-operator techniques by assuming that all variables other than the reaction coordinate equilibrate rapidly [8]. This result was first derived by expanding the rate to fourth order in J and constructing a Padé approximant [38]. It should be noted that this expression for the rate is exact for a Debye solvent with a single relaxation time [2]. In that case the operator $\hat{h}$ is a scalar and has only a single eigenmode, the calculation including only single dominant mode then becomes exact. The present procedure allows a systematic improvement of this expression. The next member of the hierarchy is obtained by taking into account two dominant eigenmodes ($M = 2$). We then have

$$K_{21}^{(2)} = \frac{2\pi|J|^2 g_0 + (2\pi|J|^2)^2 (g_0 A - g_1)}{1 + 2\pi|J|^2 A + (2\pi|J|^2)^2 B} \tag{4.21}$$

where

$$A \equiv \frac{g_1 g_2 - g_0 g_3}{g_1^2 - g_0 g_2} \tag{4.22}$$

$$B \equiv \frac{g_2^2 - g_1 g_3}{g_1^2 - g_0 g_2} \tag{4.23}$$

$K_{21}^{(1)}$ and $K_{21}^{(2)}$ will be compared in the next section. An algorithm for calculating the frequency-dependent ET rate $K_{21}(s)$ is outlined in Appendix C.

V. NUMERICAL RESULTS

We have applied the present theory to calculate the ET rates in model solvents. The following parameters were used. The total reorganization energy $\lambda \equiv \lambda_1 + \lambda_2$ is taken to be 0.1 eV and $T = 300$ K. The reaction free-energy gap, $-\Delta G^0$ is varied from 0.0, 0.05 eV (Marcus' normal region)

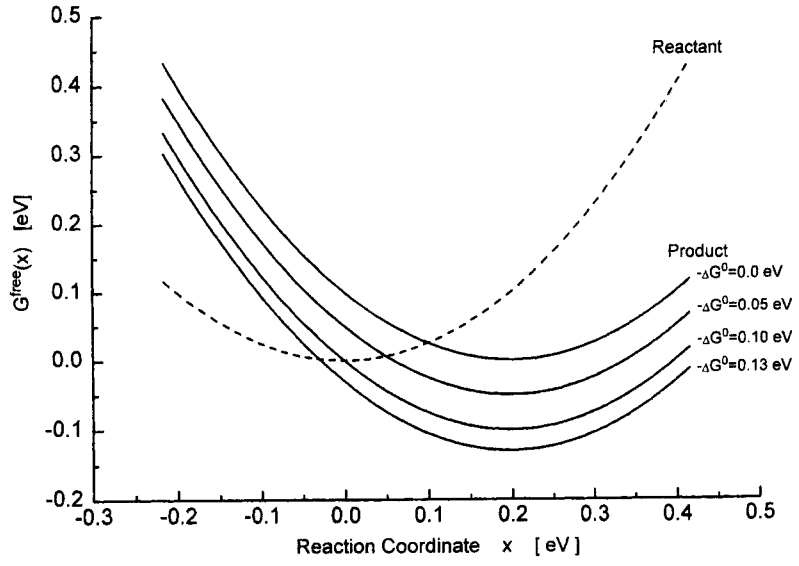

Figure 1. Free energy $G^{free}(x)$ (eV) versus reaction coordinate (eV). For different values of the free-energy gap $-\Delta G^0$ (eV), as indicated.

through 0.1 eV (activationless process) to 0.13 eV (inverted region). The free-energy curves $G_m^{free}(x)$ for these parameters are shown in Figure 1. Here $G_m^{free}(x)$ is a free energy of the mth electronic state

$$G_m^{free}(x) \equiv -k_B T \ln\left[\int \mathbf{q}\delta(x(\mathbf{q}) - x) \exp\left(-\frac{U_m(\mathbf{q})}{k_B T}\right)\right] \tag{5.1}$$

We assume two collective coordinates. The reaction coordinate is a linear combination of these two collective coordinates, and its normalized auto-correlation function is [Eq. (4.18)]

$$M(t) = \frac{\lambda_1}{\lambda} \exp(-\Lambda_1 t) + \frac{\lambda_2}{\lambda} \exp(-\Lambda_2 t) \tag{5.2}$$

The coefficients of the linear combination and time scales that appear in Eq. (5.2) are taken from the dielectric function of propanol [8] as $\lambda_1/\lambda = 0.52$, $\lambda_2/\lambda = 0.48$, $\Lambda_1^{-1} = 430\,\text{ps}$ and $\Lambda_2^{-1} = 2.12\,\text{ps}$. The numerical algorithm for solving Eq. (4.3) is described in Appendix D. In Figures 2–5 we compare the ET rates calculated using the complete multimode expression, Eq. (4.3), and the single-mode expression, Eq. (4.8). In Figures 4 and 5 we also show the ET rate calculated using the two-mode rate, Eq. (4.21). The result shows a

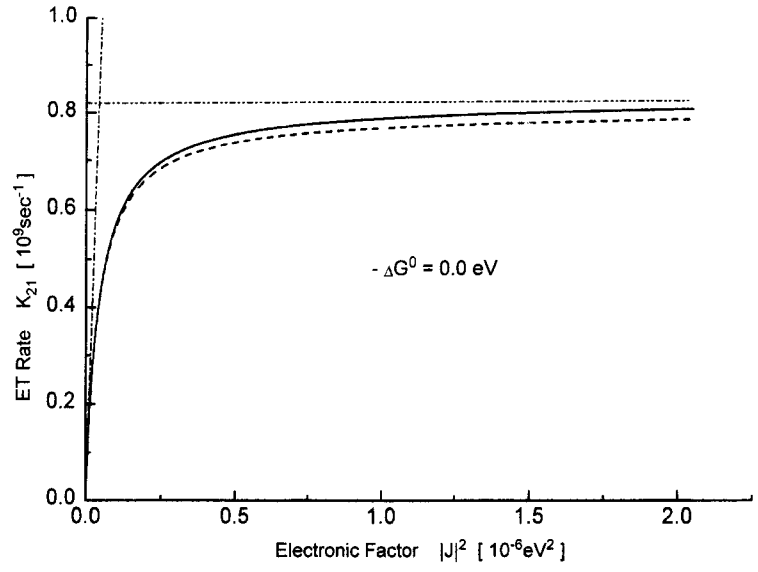

Figure 2. ET rate K_{21} versus electronic factor $|J|^2$ (eV^2). The free-energy gap $-\Delta G^0 = 0$ eV. The reorganization energies, $\lambda = 0.1$ eV, $\lambda_1 = 0.052$ eV, and $\lambda_2 = 0.048$ eV. The relaxation times, $\Lambda_1^{-1} = 430$ ps and $\Lambda_2^{-1} = 2.12$ ps. The temperature $T = 300$ K. Solid line, the complete multimode rate [Eq. (4.3)]; dashed line, the single-mode rate [Eq. (4.19)]; dash-dotted line, the nonadiabatic rate [Eq. (4.6)]; dash-dot-dotted line, the adiabatic rate [Eq. (4.7)].

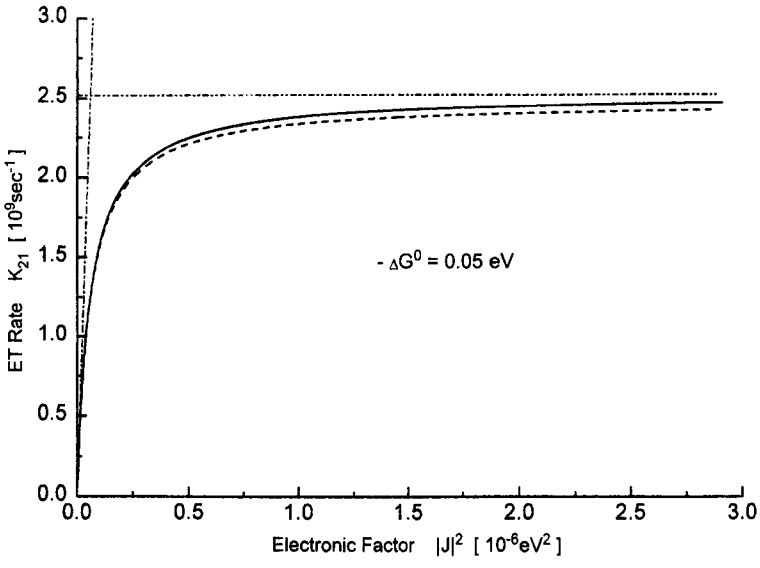

Figure 3. Same as Figure 2, but for $-\Delta G^0 = 0.05$ eV.

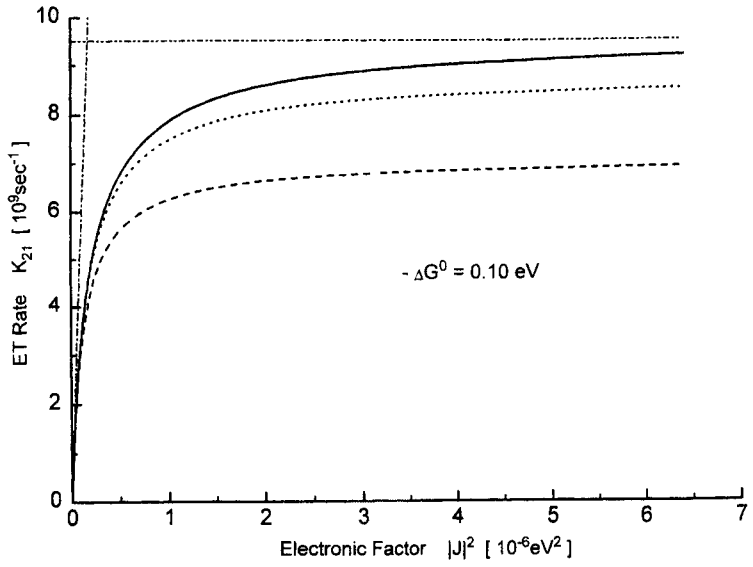

Figure 4. Same as Figure 2, but for $-\Delta G^0 = 0.10\,\text{eV}$. Dotted line, the two-mode rate [Eq. (4.21)].

$\sim 30\%$ difference between adiabatic limits of the complete multimode expression, Eq. (4.3), and the single-mode expression, Eq. (4.8), for $-\Delta G^{(0)} = 0.1\,\text{eV}$. For $-\Delta G^{(0)} = 0.13\,\text{eV}$, the difference reaches one order of magnitude. Figures 4 and 5 further illustrate how the approximation can be improved by increasing the number of dominant modes.

The difference between the complete multimode rate, Eq. (4.3), and the single-mode rate, Eq. (4.19), reflects the limitation of the assumption that all solvent variables other than the reaction coordinate equilibrate rapidly. To investigate this difference further, we varied the ratio of the two solvent relaxation time scales, Λ_2/Λ_1. We note that $K_{21}^{(1)}$ coincides with Eq. (4.3) when the two solvent relaxation time scales are the same (see Section IV). We further assumed that $\lambda_1 = \lambda_2 = 0.05\,\text{eV}$. One of the relaxation times, Λ_1^{-1}, is fixed to 1 ns. The logarithm of the ET rates calculated using the two expressions with the ratio of the two time scales, Λ_2/Λ_1, 10, 25, and 50 are shown in Figures 6, 7, and 8, respectively, versus the free-energy gap $-\Delta G^0$. As expected, the difference increases as the ratio deviates from 1. When the ratio is 25 and 50, the values of the free-energy gap $-\Delta G^0$ that gives the maximum value of the ET rate deviate considerably from the reorganization energy 0.1 eV. It is not possible to predict these values using the single-mode rate $K_{21}^{(1)}$.

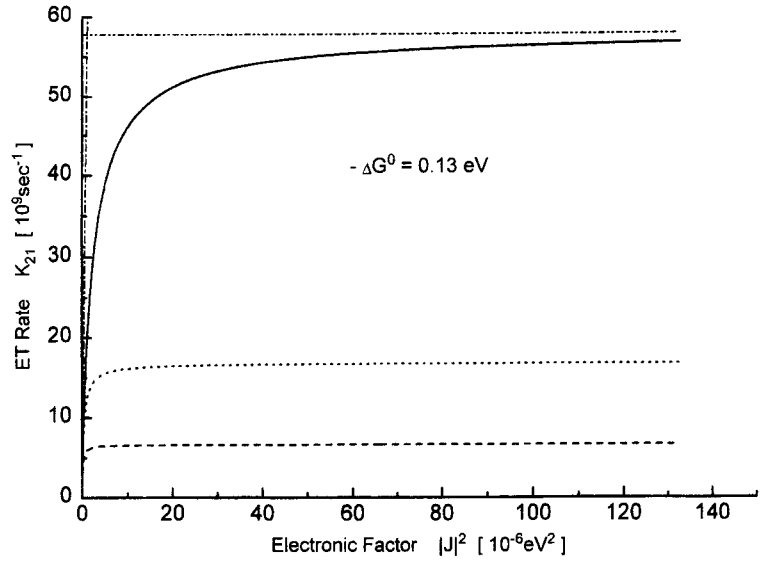

Figure 5. Same as Figure 4, but for $-\Delta G^0 = 0.13\,\text{eV}$.

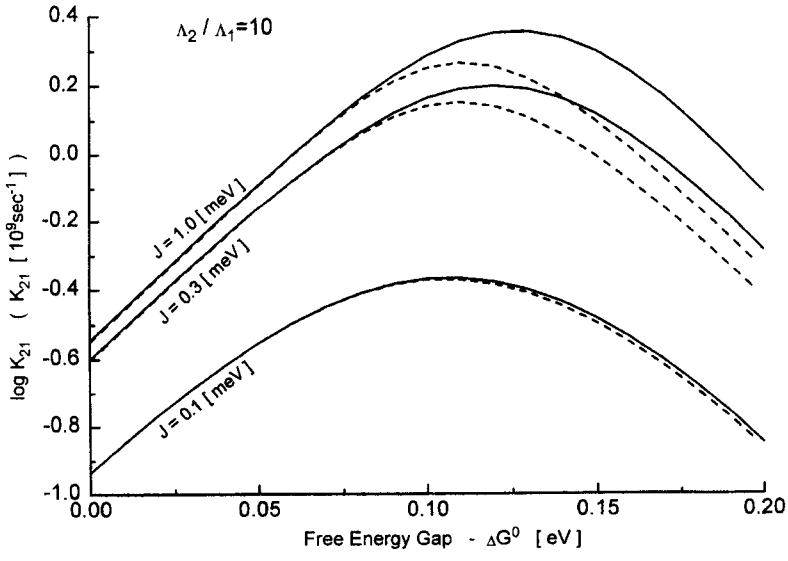

Figure 6. Logarithm of the rate $[10^9\,\text{sec}^{-1}]$ versus free-energy gap $-\Delta G^0$ (eV), for different values of the electronic coupling J, as indicated. The reorganization energy λ is 0.1 eV, and $\lambda_1 = \lambda_2 = 0.05\,\text{eV}$. The relaxation times, $\Lambda_1^{-1} = 1\,\text{ns}$ and $\Lambda_2^{-1} = 100\,\text{ps}$. The temperature $T = 300\,\text{K}$. Solid line, the complete multimode rate [Eq. (4.3)]; dashed line, the single-mode rate [Eq. (4.19)]. For the largest J the ET rate is almost in the adiabatic limit ($\Lambda_2/\Lambda_1 = 10$).

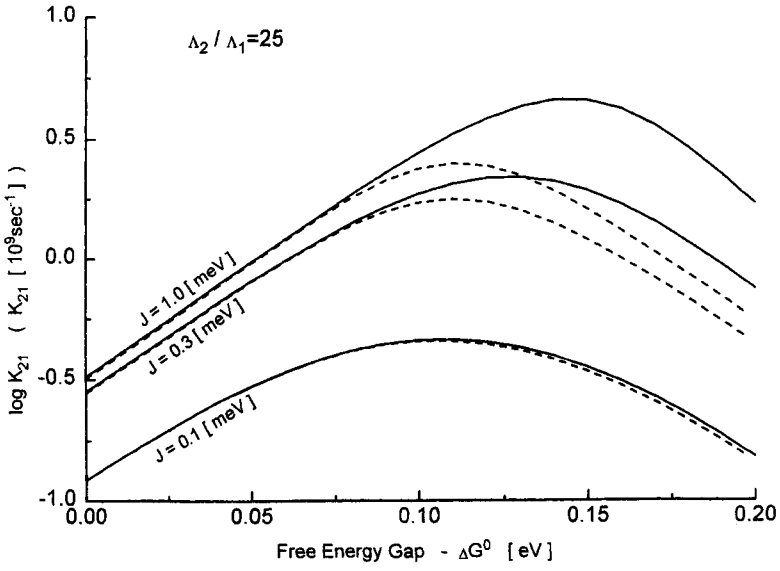

Figure 7. Same as Figure 6, but for $\Lambda_2^{-1} = 40\,\text{ps}$ ($\Lambda_2/\Lambda_1 = 25$).

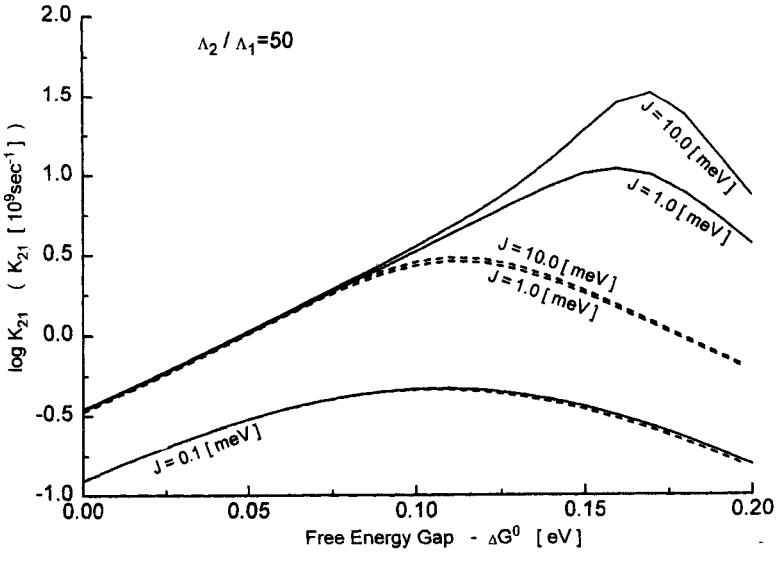

Figure 8. Same as Figure 6, but for $\Lambda_2^{-1} = 20\,\text{ps}$ ($\Lambda_2/\Lambda_1 = 50$).

VI. DISCUSSION

In this chapter we developed an algorithm for calculating ET rates in systems with complex nuclear dynamics with an arbitrary distribution of time scales. The present theory is based on the collective description of nuclear dynamics derived in [30], which treats the solvent by means of a few collective nuclear modes (NCM). The required number of collective nuclear modes depends on the form of the solvent spectral density. When the solvent can be described by a single overdamped mode, the curve-crossing manifold becomes a point and the integral equation (3.9) that describes the systems evolution can be reduced to an algebraic equation by performing a Laplace transform with respect to time. In this case Eq. (3.9) is equivalent to the equation derived by Zusman [2]. We have employed a generalization of the Lanczos algorithm [37] for inverting non-Hermitian operators [36] to solve the integral equation. The Lanczos procedure leads to a new set of effective modes (LCM), which describe collective dynamics of the system. The number of LCM may be larger or smaller than the number of NCM; the number of NCM characterizes how collective is the solvent with respect to its coupling to the electronic subsystem, whereas the number of LCM indicates how collective is the evolution of the particular observable of interest. With the larger number of NCM it is more difficult to invert the operator $\hat{h}$ in Eq. (4.3) directly, because this operator is expressed by a large matrix. This is the case where the Lanczos algorithm may become useful. To take into account M LCMs we need to calculate g_{2M-1} in Eq. (4.10); this is the most time-consuming process in the Lanczos algorithm. In this step, integrations over the collective coordinates can be carried out analytically because $g(\mathbf{x}, \mathbf{x}')$ is a Gaussian function of $\mathbf{x}$ and $\mathbf{x}'$ [Eq. (4.5)]. Consequently we only need to calculate $2M - 1$ multiple time integrations to obtain g_{2M-1}.

The Lanczos algorithm developed in this chapter is not limited to the calculation of ET rates and may be used for a complete solution of Eq. (3.9), resulting in the time evolution of the population wave packet $\rho_{mm}(\mathbf{q}, t)$ (Appendixes B and E). These wave packets can be used to calculate the time- and frequency-resolved fluorescence and the third-order nonlinear optical response (e.g., pump–probe system) of molecular aggregates and charge-transfer systems in the spectral diffusion limit [31]. The procedure for calculating these wave packets is outlined in Appendix E. This should allow the calculation of optical signals by working in the joint electronic and nuclear phase space [30,31]. When a separation of time scales exists, one can use a reduced description in the electronic or nuclear phase space alone by eliminating fast variables and incorporating them in a relaxation kernel. However, when the nuclear and electronic relaxation time scales are comparable, it is necessary to work in the joint phase space. The Lanczos

algorithm makes such a description feasible. This can have important implications for interpreting ultrafast spectroscopic measurements in molecular aggregates [39–41].

APPENDIX A: DERIVATION OF EQ. (4.3)

In this appendix we derive the ET rate for the case of two electronic states. Using the initial condition

$$\begin{pmatrix} \rho_{11}(\mathbf{q},0) \\ \rho_{22}(\mathbf{q},0) \end{pmatrix} \equiv \begin{pmatrix} \bar{\rho}_{11}^{(eq)}(\mathbf{q}) \\ 0 \end{pmatrix} \tag{A1}$$

Equation (3.9) yields

$$r(\mathbf{x},s) = \frac{1}{s}\bar{\rho}_{11}^{(eq)}(x) - \int d\mathbf{x}' \sum_{m=1}^{2} 2\pi|J|^2 G_m(\mathbf{x},\mathbf{x}';s) r(\mathbf{x}',s) \tag{A2}$$

Equation (A2) is not suitable for direct numerical computations when s is much smaller than $K_{NA} \equiv 2\pi|J|^2 \int d\mathbf{x}\, \bar{\rho}_{11}^{(eq)}$, because it includes divergent terms in the $s = 0$ limit. These terms are dominant when s is much smaller than K_{NA}. To overcome this difficulty we shall use an expansion in s utilizing the analyticity of $r(s)$ at $s = 0$. This is guaranteed by the fact that population wave packets with arbitrary initial conditions approach an equilibrium distribution at long times, and that $r(t)$ vanishes in this limit (see Appendix F). Making use of Eqs. (3.12) and (3.13), we obtain the frequency-dependent ET rate $K_{21}(s)$

$$K_{21}(s) = \frac{s2\pi|J|^2 \int d\mathbf{x}\, r(\mathbf{x},s)}{1 - P_2(\infty)^{-1} 2\pi|J|^2 \int d\mathbf{x}\, r(\mathbf{x},s)} \tag{A3}$$

where

$$P_m(\infty) \equiv \lim_{t\to\infty} P_m(t) \tag{A4}$$

$$P_m(\infty) = \frac{\exp(-\beta G_m^{free})}{\exp(-\beta G_1^{free}) + \exp(-\beta G_2^{free})} \tag{A5}$$

here G_m^{free} is a free energy of the mth electronic state, and β is an inverse of temperature T multiplied by Boltzmann factor k_B. The second equality is

proved in Appendix F. We used the detailed-balance relation to derive Eq. (A3)

$$\frac{K_{21}(s)}{K_{12}(s)} = \frac{\exp(-\beta G_2^{free})}{\exp(-\beta G_1^{free})} \tag{A6}$$

Expanding the RHS and LHS of Eq. (A2) in s, using Eq. (A3), and defining the ordinary (zero-frequency) rate

$$K_{21} \equiv \lim_{s \to +0} K_{21}(s) \tag{A7}$$

we obtain Eq. (4.3).

APPENDIX B: INVERSION OF THE KERNEL USING THE LANCZOS ALGORITHM

We derive a procedure for inverting the kernel h by identifying the relevant dominant modes. We will use the operator notation introduced in Section IV by assuming that any kernel $h(\mathbf{x}, \mathbf{x}')$ represents an operator $\hat{h}$ acting in the space of functions $r(\mathbf{x})$ on $\mathcal{M}$, which become vectors with respect to operators. This section is not restricted to the ET rate but applies to more general observables. The expectation value of an arbitrary operator $O(\mathbf{q})$ is expressed as

$$\langle O(s) \rangle = \int d\mathbf{q} \sum_{m=1}^{2} O_m(\mathbf{q}) \rho_{mm}(\mathbf{q}, s) \tag{B1}$$

Using Eqs. (E15) and (E16), we have

$$\langle O(s) \rangle = \int d\mathbf{q} \int d\mathbf{q}' \sum_{m=1}^{2} O_m(\mathbf{q}) G_m(\mathbf{q}, \mathbf{q}'; s) \bar{\rho}_{mm}(\mathbf{q}') - \int d\mathbf{x}\, \psi(\mathbf{x}, s) \hat{h}^{-1}(s) \phi(\mathbf{x}, s) \tag{B2}$$

where $\phi(\mathbf{x}, s)$ is defined by Eq. (E18) and $\psi(\mathbf{x}, s)$ is defined as

$$\psi(\mathbf{x}, s) = \int d\mathbf{q}\, [O_1(\mathbf{q}) - O_2(\mathbf{q})] \int d\mathbf{x}\, 2\pi |J|^2 \sum_{m=1}^{2} G_m(\mathbf{q}, \mathbf{x}; s) \tag{B3}$$

We develop a procedure to calculate this expectation value in Eq. (B2), the ET rate in Eq. (4.3), the frequency-dependent ET rate in Eq. (E19), and the wave-packet in Eqs. (E15) and (E16). To that end we need to calculate quantities that have a mathematically common form $W(s)$

$$W(s) \equiv \int d\mathbf{x}\, \psi(\mathbf{x}, s)\hat{h}^{-1}(s)\phi(\mathbf{x}, s) \tag{B4}$$

where we substitute $s = 0$, $\psi(\mathbf{x}) = 1$ and $\phi(\mathbf{x}) = \bar{\rho}_{11}^{(eq)}(\mathbf{x})$ for the ET rate, and $\psi(\mathbf{x}) = 1$ and $\phi(\mathbf{x}) = \bar{\rho}_{11}^{(eq)}(\mathbf{x})$ for the frequency-dependent ET rate, and Eqs. (E17) and (E18) for the wave packet.

There is an alternative way to calculate the wave packet. Using Eq. (E13), we have

$$r(\mathbf{x}', s) = \int d\mathbf{x}\, \psi(\mathbf{x}, \mathbf{x}')\hat{h}^{-1}(s)\phi(\mathbf{x}, s) \tag{B5}$$

where $\phi(\mathbf{x}, s)$ is defined by Eq. (E18) and

$$\psi(\mathbf{x}, \mathbf{x}') = \delta(\mathbf{x}' - \mathbf{x}) \tag{B6}$$

We can use Eq. (B6) instead of Eq. (E17) as $\psi(\mathbf{x}, s)$, calculate $r(\mathbf{x}, s)$, and obtain the wave packet by substituting $r(\mathbf{x}, s)$ in Eq. (3.6). This method is better because the dimensionality of $\mathbf{x}'$ is smaller than $\mathbf{q}$.

We introduce the set of eigenfunctions $e_n(\mathbf{x}, s)$ of the operator $\hat{h}(s)$ defined by Eq. (E7) with eigenvalues $\lambda_n(s)$

$$\hat{h}(s)e_n(\mathbf{x}, s) \equiv \lambda_n(s)e_n(\mathbf{x}, s) \tag{B7}$$

which can be equivalently represented by

$$\int d\mathbf{x}' h(\mathbf{x}, \mathbf{x}', s)e_n(\mathbf{x}', s) \equiv \lambda_n(s)e_n(\mathbf{x}, s) \tag{B8}$$

We also define the bra vectors $\langle e_n(s)|$ in the following way: For any function $a(\mathbf{x}, s)$ represented in a form

$$a(\mathbf{x}, s) \equiv \sum_n a_n(s)e_n(\mathbf{x}, s) \tag{B9}$$

we have

$$\langle e_n(s)|a(s)\rangle \equiv a_n(s) \tag{B10}$$

In particular we have

$$\langle e_m(s)|e_n(s)\rangle \equiv \delta_{mn} \tag{B11}$$

Using the notation above, we have

$$W(s) = \sum_{n=1}^{\infty} \frac{f_n(s)}{\lambda_n(s)} \tag{B12}$$

where

$$f_n(s) = \int d\mathbf{x}\, \psi(\mathbf{x}, s) e_n(\mathbf{x}, s) \langle e_n(s)|\phi(s)\rangle \tag{B13}$$

Using Eq. (B7), we obtain

$$\sum_{n=1}^{\infty} f_n(s)\lambda_n^m(s) = h_m(s), \qquad m = \ldots, -1, 0, 1, \ldots \tag{B14}$$

where

$$h_n(s) \equiv \int d\mathbf{x}\, \psi(\mathbf{x}, s)\hat{h}^n(s)\phi(\mathbf{x}, s) \tag{B15}$$

For brevity we hereafter omit s, and write it explicitly only in the final expressions. These equations for $m \geq 0$ may be used to calculate λ_n and f_n. For example, when we take into account M dominant eigenmodes, we use Eq. (B14) for $m = 0, 1, 2, \ldots, 2M-1$ to obtain λ_n and f_n for $n = 1, 2, \ldots, M$. This procedure generally requires the solution of an Mth-order polynomial equation. However, we can avoid this process in calculating quantities that have the common form of RHS in Eq. (B12) as a function of λ_n and f_n. Assuming M dominant modes, Eq. (B14) is recasted as

$$h_m = \sum_{n=1}^{M} f_n\lambda_n^m, \qquad m = \ldots, -1, 0, 1, \ldots \tag{B16}$$

and we define the coefficients a_n $(n = 0, 1, 2, 3, \ldots, M)$ as follows

$$a_0 \equiv -1 \tag{B17}$$

$$a_1 \equiv \sum_{i=1}^{M} \lambda_i \tag{B18}$$

$$a_2 \equiv -\sum_{i_1<i_2}^{M} \lambda_{i_1}\lambda_{i_2} \tag{B19}$$

$$a_k \equiv (-1)^{k+1} \sum_{i_1<i_2\cdots<i_k}^{M} \lambda_{i_1}\lambda_{i_2}\cdots\lambda_{i_k} \tag{B20}$$

$$a_M \equiv (-1)^{M+1}\lambda_{i_1}\lambda_{i_2}\cdots\lambda_{i_M} \tag{B21}$$

Using Eqs. (B16)–(B21), we can prove the following recursion relations

$$h_m = \sum_{n=1}^{M} h_{m-n}a_n \tag{B22}$$

$$h_m = -\frac{1}{a_M}\sum_{n=0}^{M-1} h_{m+M-n}a_n \tag{B23}$$

First we prove Eq. (B22). Substituting definitions of a_n [Eqs. (B17)–(B21)] in the RHS of Eq. (B22) and using Eq. (B16), we see that the RHS of Eq. (B22) is equal to h_m. To prove Eq. (B23), we define λ_n', h_m', and a_n'

$$\lambda_n' = \lambda_n^{-1} \tag{B24}$$

$$h_m' = \sum_{n=1}^{M} f_n\lambda_n'^m, \qquad m = \ldots, -1, 0, 1, \ldots \tag{B25}$$

$$a_1' \equiv \sum_{i=1}^{M} \lambda_i' \tag{B26}$$

$$a_2' \equiv -\sum_{i_1<i_2}^{M} \lambda_{i_1}'\lambda_{i_2}' \tag{B27}$$

$$a_k' \equiv (-1)^{k+1} \sum_{i_1<i_2\cdots<i_k}^{M} \lambda_{i_1}'\lambda_{i_2}'\cdots\lambda_{i_k}' \tag{B28}$$

$$a_M' \equiv (-1)^{M+1}\lambda_{i_1}'\lambda_{i_2}'\cdots\lambda_{i_M}' \tag{B29}$$

Using the same proof of Eq. (B22), we can show that

$$h_m' = \sum_{n=1}^{M} h_{m-n}'a_n' \tag{B30}$$

Using Eqs. (B16)–(B21) and (B25)–(B29), we have the relationships between h_m, a_n and h'_m, a'_n

$$h'_m = h_{-m} \tag{B31}$$

$$a'_n = -\frac{a_{M-n}}{a_M} \tag{B32}$$

Substituting these equations in Eq. (B30), we obtain Eq. (B23). Equation (B22) for $m = M, M+1, \ldots, 2M-1$ can be used to calculate a_n $(n = 1, 2, 3, \ldots, M)$, since in these equations h_m for $m < 0$ does not appear. Using these a_n $(n = 0, 1, 2, 3, \ldots, M)$ and Eq. (B23) for $m = -1$, we can express the RHS in Eq. (B12) as

$$W(s) = -\frac{1}{a_M} \sum_{n=0}^{M-1} h_{M-1-n} a_n \tag{B33}$$

We demonstrate this procedure by taking into account one eigenmode $(M = 1)$ and two eigenmodes $(M = 2)$. First, we calculate the RHS in Eq. (B12) by one eigenmode $(M = 1)$. In this case we only need to consider a single equation

$$h_1 = h_0 a_1 \tag{B34}$$

Using this equation, we can calculate a_1, and substituting this in Eq. (B33), we obtain the single-mode approximation

$$W(s) = \frac{h_0^2}{h_1} \tag{B35}$$

Substituting $s = 0$, $\psi(\mathbf{x}) = 1$ and $\phi(\mathbf{x}) = \bar{\rho}_{11}^{(eq)}(\mathbf{x})$ in Eqs. (B15) and (B35), we obtain the single-mode rate in Eq. (4.8). The next member of the hierarchy is obtained by taking into account two dominant eigenmodes $(M = 2)$. In this case a_1 and a_2 satisfy the equation

$$\begin{pmatrix} h_2 \\ h_3 \end{pmatrix} \equiv \begin{pmatrix} h_1 & h_0 \\ h_2 & h_1 \end{pmatrix} \begin{pmatrix} a_1 \\ a_2 \end{pmatrix} \tag{B36}$$

Solving these equations yields

$$\begin{pmatrix} a_1 \\ a_2 \end{pmatrix} \equiv \frac{1}{h_1^2 - h_0 h_2} \begin{pmatrix} h_1 & -h_0 \\ -h_2 & h_1 \end{pmatrix} \begin{pmatrix} h_2 \\ h_3 \end{pmatrix} \tag{B37}$$

Substituting in Eq. (B33), we obtain the two-mode approximation

$$W(s) = \frac{h_1^2 - h_0 h_2}{h_2^2 - h_1 h_3} \left(h_0 \frac{h_1 h_2 - h_0 h_3}{h_1^2 - h_0 h_2} - h_1 \right) \tag{B38}$$

Substituting $s = 0$, $\psi(\mathbf{x}) = 1$, and $\phi(\mathbf{x}) = \bar{\rho}_{11}^{(eq)}(\mathbf{x})$ in Eqs. (B15) and (B38), we finally obtain the two-mode rate in Eq. (4.21).

Using the above procedure, we can calculate the wave packet by substituting Eqs. (B6) and (E18) in Eq. (B15). It seems that we need to calculate the coefficients a_n $(n = 0, 1, 2, 3, \ldots, M)$ at each $\mathbf{x}'$ because of the $\mathbf{x}'$ dependence of h_n, but we can avoid this process as follows. Since the coefficients a_n $(n = 0, 1, 2, 3, \ldots, M)$ are expressed in only the eigenvalues λ_i [Eqs. (B17)–(B21)] and do not depend on $\mathbf{x}'$, we calculate these coefficients by substituting $\psi(\mathbf{x}) = 1$ in Eq. (B15) instead of Eq. (B6). We calculate $h_n(\mathbf{q}, s)$ by substituting Eqs. (B6) and (E18) in Eq. (B15). Substituting $h_n(\mathbf{q}, s)$ and the coefficients $a_n(s)$ $(n = 0, 1, 2, 3, \ldots, M)$ in Eq. (B33), we can calculate $r(\mathbf{x}, s)$. Finally, substituting $r(\mathbf{x}, s)$ in Eq. (3.6), we obtain the wave packet. Taking into account M eigenmodes, we have

$$W(\mathbf{x}', s) = -\frac{1}{a_M(s)} \sum_{n=0}^{M-1} h_{M-1-n}(\mathbf{x}', s) a_n(s) \tag{B39}$$

where

$$h_n(\mathbf{x}', s) = \int d\mathbf{x}\, \psi(\mathbf{x}, \mathbf{x}') \hat{h}^n(s) \phi(\mathbf{x}, s), \qquad n = 0, 1, \ldots, M-1 \tag{B40}$$

$$h_n(s) = \int d\mathbf{x}\, \hat{h}^n(s) \phi(\mathbf{x}, s), \qquad n = 0, 1, \ldots, 2M-1 \tag{B41}$$

$$h_m(s) = \sum_{n=1}^{M} h_{m-n}(s) a_n(s), \qquad m = M, M+1, \ldots, 2M-1 \tag{B42}$$

Here $\psi(\mathbf{x}, \mathbf{x}')$ and $\phi(\mathbf{x}, s)$ are defined by Eqs. (B6) and (E18), respectively. To calculate the function $C(s)$ in Eq. (E18) defined by Eq. (E14), we need to invert $\hat{h}^{-1}(s)$. This calculation can be done by the procedure above. Substituting Eq. (B39) in Eq. (3.6) as $r(\mathbf{x}', s)$, we obtain the M-mode wave packet.

APPENDIX C: THE FREQUENCY-DEPENDENT ET RATE

In this appendix we develop the algorithm for computing the frequency-dependent ET rate $K_{21}(s)$. We shall use the operator representation defined in Appendix B. Expanding the RHS and LHS of Eq. (A2) in s, we obtain

$$\int d\mathbf{x}\, r^{(0)}(\mathbf{x}) = \frac{P_2(\infty)}{2\pi|J|^2} \tag{C1}$$

$$r^{(0)}(\mathbf{x}) = -\frac{2\pi|J|^2}{P_2(\infty)}\, \hat{h}^{-1}\bar{\rho}_{11}^{(eq)}(\mathbf{x}) \int d\mathbf{x}\, r^{(1)}(\mathbf{x}) \tag{C2}$$

$$r^{(n)}(\mathbf{x}) = -2\pi|J|^2\hat{h}^{-1}\sum_{k=0}^{n-1} \hat{g}^{(n-k)}r^{(k)}(\mathbf{x}) - \frac{2\pi|J|^2}{P_2(\infty)}\, \hat{h}^{-1}\bar{\rho}_{11}^{(eq)}(\mathbf{x}) \int d\mathbf{x}\, r^{(n+1)}(\mathbf{x}), \qquad n = 1, 2, \ldots \tag{C3}$$

where $r^{(k)}(\mathbf{x})$ and $\hat{g}^{(k)}$ are defined as

$$r(\mathbf{x}, s) \equiv \sum_{k=0}^{\infty} s^k r^{(k)}(\mathbf{x}) \tag{C4}$$

$$\hat{g}^{(k)} \equiv \int_0^{\infty} dt\, \frac{(-t)^k}{k!} \sum_{m=1}^{2} [G_m(\mathbf{x}, \mathbf{x}', t) - \bar{\rho}_{mm}^{(eq)}(\mathbf{x})] \tag{C4}$$

Here $\hat{g}^{(0)}$ is the same as the operator representation of $g(\mathbf{x}, \mathbf{x}')$ in Eq. (4.5), $\hat{g}$, and $\hat{h}$ is the operator representation of $h(\mathbf{x}, \mathbf{x}')$ in Eq. (4.4). Here we used the analyticity of $r(\mathbf{x}, s)$ at $s = 0$. This is guaranteed since a population wave packet with arbitrary initial condition attains an equilibrium distribution at long times, and in this limit $r(\mathbf{x}, t)$ is zero (see Appendix F). Using Eqs. (C2) and (C3), we have

$$\int d\mathbf{x}\, r^{(1)}(\mathbf{x}) = -\frac{\int d\mathbf{x}\, r^{(0)}(\mathbf{x})}{[2\pi|J|^2/P_2(\infty)] \int d\mathbf{x}\hat{h}^{-1}\bar{\rho}_{11}^{(eq)}(\mathbf{x})} \tag{C6}$$

$$\int d\mathbf{x}\, r^{(n+1)}(\mathbf{x}) = \frac{\int d\mathbf{x}\, r^{(n)}(\mathbf{x}) + 2\pi|J|^2 \int d\mathbf{x}\, \hat{h}^{-1} \sum_{k=0}^{n-1} \hat{g}^{(n-k)}r^{(k)}(\mathbf{x})}{[2\pi|J|^2/P_2(\infty)] \int d\mathbf{x}\, \hat{h}^{-1}\bar{\rho}_{11}^{(eq)}(\mathbf{x})}, \qquad n = 1, 2, \ldots \tag{C7}$$

Since Eqs. (C1)–(C7) do not include divergent terms at $s = 0$, they can be used to calculate $r^{(k)}(\mathbf{x})$ numerically using the following procedure. First, substituting Eq. (C1) in Eqs. (C2) and (C6), we obtain $r^{(0)}(\mathbf{x})$ and $\int d\mathbf{x}\, r^{(1)}(\mathbf{x})$. Second, substituting $r^{(0)}(\mathbf{x})$ and $\int d\mathbf{x}\, r^{(1)}(\mathbf{x})$ in Eqs. (C3) and (C7) for $n = 1$, we can obtain $r^{(1)}(\mathbf{x})$ and $\int d\mathbf{x}\, r^{(2)}(\mathbf{x})$. Generally at the $(n+1)$-th step, substituting $r^{(k)}(\mathbf{x})(k < n)$ and $\int d\mathbf{x}\, r^{(n)}(\mathbf{x})$, in Eqs. (C3) and (C7) we can calculate $r^{(n)}(\mathbf{x})$ and $\int d\mathbf{x}\, r^{(n+1)}(\mathbf{x})$. In Section IV we used this first step and calculated the ET rate in zero-frequency limit. Substituting Eqs. (C1) and (C3) in Eq. (A3), the frequency-dependent ET rate is given by

$$K_{21}(s) = -P_2(\infty)\frac{\sum_{k=0}^{\infty} s^k \int d\mathbf{x}\, r^{(k)}(\mathbf{x})}{\sum_{k=1}^{\infty} s^{k-1} \int d\mathbf{x}\, r^{(k)}(\mathbf{x})} \tag{C8}$$

In particular, in the zero-frequency limit we recover Eq. (4.3).

APPENDIX D: NUMERICAL SOLUTION OF EQS. (4.3), (4.8), AND (4.21)

In this appendix we describe the numerical algorithm for computing the ET rate using Eqs. (4.3) and (4.19). We first calculate $h(\mathbf{x}, \mathbf{x}')$ numerically using Eqs. (4.4) and (4.5). Second we calculate the inverse of $h(\mathbf{x}, \mathbf{x}')$, $h^{-1}(\mathbf{x}, \mathbf{x}')$, and the rate K_{21} using Eq. (4.3). It should be noted that using $\mathbf{x}$ in the numerical calculation is not convenient, because the Green function $G_m(\mathbf{x}, \mathbf{x}', t)$ becomes a delta function at $t = 0$. To overcome this difficulty we use different coordinates. The parameters used in the calculations are the temperature, T, the inverses of relaxation times of the collective coordinates Λ_α, and $d_{\alpha,m}$.

We perform a linear transformation of the collective coordinates q_α as coordinates of $\mathbf{x}$, and take the reaction coordinate $x(\mathbf{q})$ as the Nth coordinate of $\mathbf{x}$

$$\mathbf{x} \equiv \mathbf{A}\mathbf{q} \tag{D1}$$

$$x_N \equiv x(\mathbf{q}) \tag{D2}$$

where $\mathbf{A}$ is an $N \times N$ matrix. Using Eqs. (3.8), (D1), and (D2), we have

$$\int d\mathbf{x} \cdots = |det\, \mathbf{A}|^{-1} \int_{x_{N=0}} \prod_{i=1}^{N-1} dx_i \cdots \tag{D3}$$

We define basis function $u_n(\mathbf{x})$ $(n = 1, 2, 3, \ldots, N_u)$ as

$$u_n(\mathbf{x}) \equiv |det\, \mathbf{A}| \prod_{i=1}^{N-1} \sqrt{\frac{a_i}{\pi}} \exp[-a_i(x_i - b_{i,n})] \tag{D4}$$

$$b_{i,n} \equiv \Delta b_i \left(n - \frac{N_u}{2} \right) \tag{D5}$$

We further define a vector $\mathbf{f}$ and a matrix $\mathbf{F}$ that correspond to $f(\mathbf{x})$ and $F(\mathbf{x}, \mathbf{x}')$, respectively, as

$$\sum_n u_n(\mathbf{x})[\mathbf{f}]_n \equiv f(\mathbf{x}) \tag{D6}$$

$$\sum_n u_n(\mathbf{x})[\mathbf{F}]_{nn'} \equiv \int d\mathbf{x}'\, F(\mathbf{x}, \mathbf{x}') u_{n'}(\mathbf{x}') \tag{D7}$$

we then have,

$$\sum_n u_n(\mathbf{x})[\mathbf{Ff}]_n \equiv \int d\mathbf{x}'\, F(\mathbf{x}, \mathbf{x}') f(\mathbf{x}') \tag{D8}$$

$$\sum_n u_n(\mathbf{x})[\mathbf{F}^{-1}\mathbf{f}]_n \equiv \int d\mathbf{x}'\, F^{-1}(\mathbf{x}, \mathbf{x}') f(\mathbf{x}') \tag{D9}$$

$$\mathbf{f} \equiv \mathbf{S}^{-1}\mathbf{f}' \tag{D10}$$

$$\mathbf{F} \equiv \mathbf{S}^{-1}\mathbf{F}' \tag{D11}$$

where

$$[\mathbf{f}']_n \equiv \int d\mathbf{x}\, u_n(\mathbf{x}) f(\mathbf{x}) \tag{D12}$$

$$[\mathbf{F}']_{nn'} \equiv \int d\mathbf{x} \int d\mathbf{x}'\, u_n(\mathbf{x}) F(\mathbf{x}, \mathbf{x}') u_{n'}(\mathbf{x}') \tag{D13}$$

$$[\mathbf{S}]_{nn'} \equiv \int d\mathbf{x}\, u_n(\mathbf{x}) u_{n'}(\mathbf{x}) \tag{D14}$$

We now describe the numerical scheme. Using Eq. (D11), we have

$$\mathbf{g} \equiv \mathbf{S}^{-1}\mathbf{g}' \tag{D15}$$

where

$$[\mathbf{g}']_{nn'} \equiv \int d\mathbf{x} \int_0^\infty dt \int d\mathbf{x}' \, u_{n''}(\mathbf{x}) g(\mathbf{x}, \mathbf{x}', t) u_{n'}(\mathbf{x}') \tag{D16}$$

Here the $\mathbf{x}'$ integral can be obtained analytically. In Eq. (D16) $g(\mathbf{x}, \mathbf{x}', t)$ has a component that goes to the delta function at $t = 0$, but it can be integrated analytically. Using Eq. (4.4), we have

$$\mathbf{h} \equiv \mathbf{1} + 2\pi |J|^2 \mathbf{g} \tag{D17}$$

Using Eq. (4.3), we have

$$K_{21} = 2\pi |J|^2 \sum_n [\mathbf{h}^{-1} \bar{\mathbf{p}}_{11}^{(eq)}]_n \tag{D18}$$

where

$$\bar{\mathbf{p}}_{11}^{(eq)} \equiv \mathbf{S}^{-1} \mathbf{p}_{11}^{(eq)'} \tag{D19}$$

$$[\bar{\mathbf{p}}_{11}^{(eq)'}]_n \equiv \int d\mathbf{x} \, u_n(\mathbf{x}) \bar{\rho}_{11}^{(eq)}(\mathbf{x}) \tag{D20}$$

The ET rates in Eqs. (4.8) and (4.21) are calculated in the same manner.

APPENDIX E: SOLUTION OF EQ. (2.9): DENSITY-MATRIX NUCLEAR WAVE PACKETS

In this appendix we show how the nuclear wave packets may be calculated. We shall use the operator representation defined in Appendix B. Since we will use this wave packet to calculate expectation values of arbitrary operators, we assume an arbitrary initial condition

$$\begin{pmatrix} \rho_{11}(\mathbf{q}, 0) \\ \rho_{22}(\mathbf{q}, 0) \end{pmatrix} \equiv \begin{pmatrix} \bar{\rho}_{11}(\mathbf{q}) \\ \bar{\rho}_{22}(\mathbf{q}) \end{pmatrix} \tag{E1}$$

Equation (3.9) then yields

$$r(\mathbf{x}, s) = S(\mathbf{x}, s) - \int d\mathbf{x}' \sum_{m=1}^{2} 2\pi |J|^2 G_m(\mathbf{x}, \mathbf{x}'; s) r(\mathbf{x}', s) \tag{E2}$$

where

$$S(\mathbf{x},s) \equiv \int d\mathbf{q}\, G_1(\mathbf{x},\mathbf{q};s)\bar{\rho}_{11}(\mathbf{q}) - \int d\mathbf{q}\, G_2(\mathbf{x},\mathbf{q};s)\bar{\rho}_{22}(\mathbf{q}) \tag{E3}$$

$S(\mathbf{x},s)$ and $G_m(\mathbf{x},\mathbf{x}';s)$ in Eq. (E2) contain divergent terms in $s=0$ limit. To remove these terms we expand both sides of Eq. (E2) in s. Taking terms in s^{-1}, we have

$$\int d\mathbf{x}\, r^{(0)}(\mathbf{x}) = \frac{P_1(0)P_2(\infty) - P_1(\infty)P_2(0)}{2\pi|J|^2} \tag{E4}$$

where $r^{(k)}(\mathbf{x})$ is defined by Eq. (C4), and $P_m(t)$ is defined by Eq. (3.11). Substituting Eq. (E4) in Eq. (E2), we obtain

$$r(\mathbf{x},s) = \hat{h}^{-1}(s)\left(S_0(\mathbf{x},s) - \frac{2\pi|J|^2}{P_2(\infty)}\,\bar{\rho}_{11}^{(eq)}(\mathbf{x})\,\frac{\int d\mathbf{x}\, r(\mathbf{x},s) - \int d\mathbf{x}\, r^{(0)}(\mathbf{x})}{s}\right) \tag{E5}$$

where

$$\hat{g}(s) \equiv \int_0^\infty dt\, e^{-st} \sum_{m=1}^{2} [G_m(\mathbf{x},\mathbf{x}',t) - \bar{\rho}_{mm}^{(eq)}(\mathbf{x})] \tag{E6}$$

$$\hat{h}(s) \equiv 1 + 2\pi|J|^2\hat{g}(s) \tag{E7}$$

$$S(\mathbf{x},s) \equiv \sum_{k=-1}^{\infty} s^k S^{(k)}(\mathbf{x}) \tag{E8}$$

$$S_0(\mathbf{x},s) \equiv S(\mathbf{x},s) - s^{-1}S^{(-1)}(\mathbf{x}) \tag{E9}$$

Considering that $\lim_{t\to\infty} G_m(\mathbf{x},\mathbf{x}',t) = \bar{\rho}_{mm}^{(eq)}(\mathbf{x})$, we have

$$\begin{aligned} S_0(x,s) = \int d\mathbf{q}\, \{&[G_1(\mathbf{x},\mathbf{q};s) - s^{-1}\bar{\rho}_{11}^{(eq)}(\mathbf{x})]\bar{\rho}_{11}(\mathbf{q}) \\ &- [G_2(\mathbf{x},\mathbf{q};s) - s^{-1}\bar{\rho}_{22}^{(eq)}(\mathbf{x})]\bar{\rho}_{22}(\mathbf{q})\} \end{aligned} \tag{E10}$$

Integrating both sides of Eq. (E5) over the crossing manifold, we have

$$\int d\mathbf{x}\, r(\mathbf{x},s) = \frac{\int d\mathbf{x}\, \hat{h}^{-1}(s)[sS_0(\mathbf{x},s) + c\bar{\rho}_{11}^{(eq)}(\mathbf{x})]}{s + [2\pi|J|^2/P_2(\infty)] \int d\mathbf{x}\, \hat{h}^{-1}(s)\bar{\rho}_{11}^{(eq)}(\mathbf{x})} \tag{E11}$$

where

$$c = \frac{P_1(0)P_2(\infty) - P_1(\infty)P_2(0)}{P_2(\infty)} \tag{E12}$$

Substituting Eq. (E11) in Eq. (E5), we have

$$r(\mathbf{x}, s) = \hat{h}^{-1}(s)[S_0(\mathbf{x}, s) + C(s)\bar{\rho}_{11}^{(eq)}(\mathbf{x})] \tag{E13}$$

where

$$C(s) = \left(c - \frac{2\pi|J|^2}{P_2(\infty)} \int d\mathbf{x}\, \hat{h}^{-1}(s) S_0(\mathbf{x}, s)\right) \Big/ \left(s + \frac{2\pi|J|^2}{P - 2(\infty)} \int d\mathbf{x}\, \hat{h}^{-1}(s)\bar{\rho}_{11}^{(eq)}(\mathbf{x})\right) \tag{E14}$$

Using Eq. (3.6), we obtain the frequency-dependent wave packet

$$\rho_{11}(\mathbf{q}, s) = \int d\mathbf{q}'\, G_1(\mathbf{q}, \mathbf{q}'; s)\bar{\rho}_{11}(\mathbf{q}') - \int d\mathbf{x}\, \psi(\mathbf{x}, \mathbf{q}, s)\hat{h}^{-1}(s)\phi(\mathbf{x}, s) \tag{E15}$$

$$\rho_{22}(\mathbf{q}, s) = \int d\mathbf{q}'\, G_2(\mathbf{q}, \mathbf{q}'; s)\bar{\rho}_{22}(\mathbf{q}') + \int d\mathbf{x}\, \psi(\mathbf{x}, \mathbf{q}, s)\hat{h}^{-1}(s)\phi(\mathbf{x}, s) \tag{E16}$$

where

$$\psi(\mathbf{x}, \mathbf{q}, s) = 2\pi|J|^2 \sum_{m=1}^{2} G_m(\mathbf{q}, \mathbf{x}; s) \tag{E17}$$

$$\phi(\mathbf{x}, s) = S_0(\mathbf{x}, s) + C(s)\bar{\rho}_{11}^{(eq)}(\mathbf{x}) \tag{E18}$$

We next derive another expression of the frequency-dependent rate using Eq. (E11). Substituting Eq. (E11) in Eq. (A3) and using the initial condition Eq. (A1), we have

$$K_{21}(s) = 2\pi|J|^2 \int d\mathbf{x}\, \hat{h}^{-1}(s)\bar{\rho}_{11}^{(eq)}(\mathbf{x}) \tag{E19}$$

In particular, by substituting $s = 0$ in this equation, we recover Eq. (4.3).

In summary, we outline the procedure for calculating the evolution of population wave packets using the Lanczos algorithm. The procedure involves the following steps:

1. Given the initial values of population wave packets $\bar{\rho}_{11}(\mathbf{q})$ and $\bar{\rho}_{22}(\mathbf{q})$, we evaluate the function $S_0(\mathbf{x}, s)$ using Eq. (E10). The Green functions

$G_m(\mathbf{q},\mathbf{q}';t)$ in the time domain are defined by Eqs. (3.3)–(3.5). The Green functions $G_m(\mathbf{q},\mathbf{q}';s)$ in Eq. (E10) are obtained from $G_m(\mathbf{q},\mathbf{q}';t)$ by applying the Laplace transform defined by Eq.(3.17).

2. Choose the number of LCM by fixing an integer number M and calculating a set of functions $h_n(s)(n=0,1,2,3,\ldots,2M-1)$ using Eq. (B15) with $\psi(\mathbf{x},s)=1$ and $\phi(\mathbf{x},s)=[2\pi|J|^2/P_2(\infty)]\bar{\rho}_{11}^{(eq)}(\mathbf{x})$, where $P_2(\infty)$ is given by Eq. (A5) and $\bar{\rho}_{11}^{(eq)}(\mathbf{x})$ can be found from Eq. (3.16). The operator $\hat{h}(s)$ in Eq. (B15) is defined by Eqs. (E6) and (E7).

3. Substitute the calculated values of $h_n(s)$ into Eq. (B22). By solving these equations for a_n, we obtain a set of functions $a_n(s)$ $(n=1,2,3,\ldots,M)$; we also set $a_0\equiv -1$.

4. Calculate the function $W(s)$ by substituting $h_n(s)$ and $a_n(s)$ calculated on steps (2) and (3) in Eq. (B33).

5. Repeat steps (2)–(4) but using $\tilde{\phi}(\mathbf{x},s)=[2\pi|J|^2/P_2(\infty)]S_0(\mathbf{x},s)$ instead $\phi(\mathbf{x},s)$ defined on step (2), where $S_0(\mathbf{x},s)$ is defined on step (1). This yields another set of functions $\tilde{h}_n(s)$, $\tilde{a}_N(s)$, and $\tilde{W}(s)$.

6. Calculate the function $C(s)$ introduced by Eq. (E14) using the following expression

$$C(s)=\frac{c-\tilde{W}(s)}{s+W(s)} \tag{E20}$$

where c is given by Eq. (E12). Note that $\tilde{W}(s)$ and $W(s)$ represent the second terms in the numerator and denominator in the RHS of Eq. (E14) calculated using the Lanczos algorithm.

7. Repeat steps (2) and (3) using $\phi'(\mathbf{x},s)=S_0(\mathbf{x},s)+C(s)\bar{\rho}_{11}^{(eq)}(\mathbf{x})$ instead of $\phi(\mathbf{x},s)$ defined on step (2); this yields a set of functions $h_n'(s)$ and $a_n'(s)$.

8. Calculate the frequency-dependent wave packets $h_n(\mathbf{x}'.s)$ $(n=0,1,2,3,\ldots,M-1)$ by substituting $\phi'(\mathbf{x},s)$ defined on step (7) instead of $\phi(\mathbf{x},s)$ into Eq. (B40) and setting $\psi(\mathbf{x},\mathbf{x}')=\delta(\mathbf{x}'-\mathbf{x})$.

9. Calculate a frequency-dependent wave packet $W(\mathbf{x}',s)$ using Eq. (B39).

10. Time-dependent population wave packets are obtained by applying the inverse Laplace transform to Eq. (3.6) for two electronic levels and substituting $W(\mathbf{x}',s)$ for the Laplace transform of $r(\mathbf{x}',s)$

$$\rho_{mm}(\mathbf{q},t)=\int d\mathbf{q}'\,G_m(\mathbf{q},\mathbf{q}';t)\bar{\rho}_{mm}(\mathbf{q}') + (-1)^m 2\pi|J|^2\int_C\frac{ds}{2\pi i}\,e^{st}\int d\mathbf{x}\,G_m(\mathbf{q},\mathbf{x};s)W(\mathbf{x},s) \tag{E21}$$

where C is the standard contour involved in the inverse Laplace transform

[42]. The procedure can be repeated with increasing the number M of LCM until satisfactory convergence is reached.

APPENDIX F: EQUILIBRATION OF POPULATION WAVE PACKETS

In this appendix we show that the population wave packets satisfying the equation of motion (3.1) with arbitrary initial conditions reach thermal equilibrium at long times. Our proof goes as follows: We first give a explicit form of the equilibrium wave packet, $\rho^{(eq)}(\mathbf{q})$, and show that $L\rho^{(eq)} = 0 (L \equiv L^{(0)} + L^{(1)})$. We next define an entropy functional of the population wave packet, $S[\rho]$, and prove that $dS[\rho]/dt > 0$ for $\rho \neq \rho^{(eq)}$, and that $dS[\rho]/dt = 0$ for $= \rho^{(eq)}$. These two results imply that a population wave packet with arbitrary initial condition tends to $\rho^{(eq)}$ at long times.

We define $\rho^{(eq)}(\mathbf{q})$ as

$$[\rho^{(eq)}(\mathbf{q})]_m = e^{-\beta[U_m(\mathbf{q}) - G^{free}]} \tag{F1}$$

where the free energy G^{free} is defined as

$$e^{-\beta G^{free}} \equiv \sum_m e^{-\beta G_m^{free}} \tag{F2}$$

$$e^{-\beta G_m^{free}} \equiv \int d\mathbf{q}\, e^{-\beta U_m} \tag{F3}$$

Using Eqs. (2.9), (2.12), (3.1), and (F1), we can easily verify that

$$L^{(0)}\rho^{(eq)} = 0 \tag{F4}$$

Using Eqs. (2.9), (3.1), and (F1), we obtain

$$[L^{(1)}\rho^{(eq)}]_m = -\sum_{m'} [K_{m'm}(\mathbf{q})\rho_{mm}^{(eq)} - K_{mm'}(\mathbf{q})_{m'm'}^{(eq)}] \tag{F5}$$

$$= 0 \tag{F6}$$

Here we used the relation $x\delta(x) = 0$. In fact, to obtain Eq. (F6) we need only the detailed-balance principle in the local form

$$\frac{K_{m'm}(\mathbf{q})}{K_{mm'}(\mathbf{q})} = \frac{\rho_{m'm'}^{(eq)}(\mathbf{q})}{\rho_{mm}^{(eq)}(\mathbf{q})} \tag{F7}$$

Equation (2.10) is the limit of one of the functions, $K_{m'm(\mathbf{q})}$ that satisfy this principle, Eq. (F7). Using Eqs. (F4) and (F6), we can show that $L\rho^{(eq)} = 0$.

We next define the functional $S[\rho]$

$$S[\rho] \equiv -k_B T \sum_m \int d\mathbf{q}\, \rho_{mm} \ln \frac{\rho_{mm}}{N_0 \rho_{mm}^{(eq)}} \tag{F8}$$

where N_0 is the number of the states of the entire system (including the heat bath that is made out of the eliminated degrees of freedom) when it has the energy that corresponds to temperature T. This functional represents the entropy of the entire system assuming that the bath is completely equilibrated. In the following proof we need only the simplified functional $S'[\rho]$

$$S'[\rho] \equiv -\sum_m \int d\mathbf{q}\, \rho_{mm} \ln \frac{\rho_{mm}}{\rho_{mm}^{(eq)}} \tag{F9}$$

Differentiating the functional $S'[\rho]$ with respect to t and recasting, we obtain

$$\frac{dS'[\rho]}{dt} \equiv i \sum_m \int d\mathbf{q} \left(L_{mm}^{(0)} \rho_{mm} + \sum_{m'} L_{mm'}^{(1)} \rho_{m'm'} \right) \ln \frac{\rho_{mm}}{\rho_{mm}^{(eq)}} \tag{F10}$$

We can easily prove that the first term of Eq. (F10) satisfies the inequality

$$i \int d\mathbf{q}\, (L_{mm}^{(0)} \rho_{mm}) \ln \frac{\rho_{mm}}{\rho_{mm}^{(eq)}} \geq 0 \text{ (equality for } \rho_{mm} = \rho_{mm}^{(eq)}) \tag{F11}$$

The second term is

$$i \sum_m \int d\mathbf{q} \left(\sum_{m'} L_{mm'}^{(1)} \rho_{m'm'} \right) \ln \frac{\rho_{mm}}{\rho_{mm}^{(eq)}} \tag{F12}$$

$$\equiv \sum_{m<m'} \int d\mathbf{q}\, [K_{m'm}(\mathbf{q}) \rho_{mm} - K_{mm'}(\mathbf{q}) \rho_{m'm'}] \left(\ln \frac{\rho_{mm}}{\rho_{mm}^{(eq)}} - \ln \frac{\rho_{m'm'}}{\rho_{m'm'}^{(eq)}} \right) \tag{F13}$$

$$\geq 0 \text{ (equality for } \rho = \rho^{(eq)}) \tag{F14}$$

where we used Eqs. (2.10) and (F1). To obtain the inequality Eq. (F14) we need only the detailed-balance principle in the local form again. Equations

(F11) and (F14) result in

$$\frac{dS'[\rho]}{dt} \geq 0 \text{ (equality for } \rho = \rho^{(eq)}) \tag{F15}$$

ACKNOWLEDGMENTS

We gratefully acknowledge the support of the Japan Society for the Promotion of Science, the National Science Foundation, and the U.S. Air Force Office of Scientific Research. We wish to thank Sergei Tretiak for most useful discussions.

REFERENCES

1. R. A. Marcus, *J. Chem. Phys.* **24**, 966 (1956); **24**, 979 (1956).
2. L. D. Zusman, *Chem. Phys.* **49**. 295 (1980).
3. J. M. Jean, R. A. Friesner, and G. R. Fleming, *J. Chem. Phys.* **96**, 5827 (1992).
4. M. A. Kahlow, T. J. Kang, and P. F. Barbara, *J. Chem. Phys.* **91**, 6452 (1987).
5. J. T. Hynes, *Annu. Rev. Phys. Chem.* **36**, 573 (1985).
6. I. Rips and J. Jortner, *J. Chem. Phys.* **87**, 2090 (1987).
7. A. Garg, J. N. Onuchic, and V. Ambegaokar, *J. Chem. Phys.* **83**, 4491 (1985).
8. M. Sparpaglione and S. Mukamel, *J. Chem. Phys.* **88**, 3263 (1988); *ibid.* **88**, 4300 (1988); *J. Phys. Chem.* **91**, 39383 (1987).
9. N. R. Kestner, J. Logan, and J. Jortner, *J. Phys. Chem.* **78**, 2148 (1974); J. Ulstrup and J. Jortner, *J. Chem. Phys. Chem.* **63**, 4358 (1975).
10. H. Sumi and R. A. Marcus, *J. Chem. Phys.* **84**, 4894 (1986).
11. H. Sumi, *J. Phys. Chem.* **95**, 3334 (1991).
12. N. Gayathri and B. Bagchi, *J. Phys. Chem.* **100**, 3056 (1996).
13. G. C. Walker, E. Akesson, A. E. Johnson, N. E. Levinger, and P. F. Barbara, *J. Phys. Chem.* **96**, 3728 (1992).
14. E. Akesson, A. E. Johnson, N. E. Levinger, G. C. Walker, T. P. DuBruil, and P. F. Barbara, *J. Chem. Phys.* **96**, 7859 (1992).
15. A. E. Johnson, N. E. Levinger, W. Jarzeba, R. E. Schleif, D. A. V. Kliner, and P. F. Barbara, *Chem. Phys.* **176**, 555 (1992).
16. H. Kandori, K. Kemnitz, and K. Yoshihara, *J. Phys. Chem.* **96**, 8042 (1992).
17. T. Kobayashi, Y. Takagi, H. Kandori, K. Kemnitz, and K. Yoshihara, *Chem. Phys. Lett.* **180**, 416 (1991).
18. Y. Nagasawa, A. P. Yartsev, K. Tominaga, A. E. Johnson, and K. Yoshihara, *J. Chem. Phys.* **101**, 5717 (1996).
19. T. Joo, Y. Jia, and G. R. Fleming, *J. Chem. Phys.* **102**, 4063 (1995).
20. P. Vohringer, D. C. Arnett, T. S. Yang, and N. F. Scherer, *Chem. Phys. Lett.* **237**, 387 (1995).
21. P. Vohringer, D. C. Arnett, R. A. Westervelt, M. J. Feldstein, and N. F. Scherer, *J. Chem. Phys.* **102**, 4027 (1995).

22. M. S. Pshenichnikov, K. Duppen, and D. A. Wiersma, *Phys. Rev. Lett.* **74**, 674 (1995).
23. W. P. de Boeij, M. S. Pshenichnikov, K. Duppen, and D. A. Wiersma, *Chem. Phys. Lett.* **224**, 243 (1994).
24. M. Cho, M. Du, N. Scherer, G. Fleming, and S. Mukamel, *J. Chem. Phys.* **99**, 2410 1993).
25. D. McMorrow, N. Thantu, J. S. Melinger, S. K. Kim, and W. T. Lotshaw, *J. Phys. Chem.* **100**, 10389 (1996).
26. D. McMorrow and W. T. Lotshaw, *J. Phys. Chem.* **95**, 10395 (1991).
27. S. Ruhman and K. A. Nelson, *J. Chem. Phys.* **94**, 859 (1991).
28. K. Tominaga and K. Yoshihara, *J. Chem. Phys.* **104**, 1159 (1996).
29. A. Tokmakov and G. R. Fleming, *J. Chem. Phys.* **106**, 2569 (1997).
30. V. Chernyak and S. Mukamel, *J. Chem. Phys.* **105**, 4565 (1996).
31. S. Mukamel, *Principles of Nonlinear Optical Spectroscopy*, Oxford, New York, 1995.
32. Y. Tanimura and R. Kubo, *J. Phys. Soc. Jpn.* **58**, 101 (1989); Y. Tanimura and S. Mukamel, *J. Chem. Phys.* **101**, 3049 (1994).
33. A. O. Caldeira and A. J. Legett, *Phys. Status Solidi A* **121**, 587 (1983).
34. A. Carg, J. N. Onuchic, and V. Ambegaokar, *J. Chem. Phys.* **83**, 4491 (1985).
35. R. Zwanzig, *Statistical Mechanics of Irreversibility*, Vol. 3 of Lectures in Theoretical Physics, Interscience, New York, 1961.
36. T. Meier and S. Mukamel, *Phys. Rev. Lett.* **77**, 3471 (1996); T. Meier, S. Tretiak, V. Chernyak, and S. Mukamel, *Phys. Rev. B*, **55**. 4960 (1997); S. Tretiak, V. Chernyak, and S. Mukamel, *J. Chem. Phys.* **105**, 8914 (1996).
37. J. K. Cullum and R. A. Willoughby, *J. Comp. Phys.* **44**, 329 (1981); T. J. Park and J. C. Light, *J. Chem. Phys.* **85**, 10 (1986); C. Leforestier, R. H. Bisseling, C. Cerjan, M. D. Feit, R. Friesner, A. Guldberg, A. Hammerich, G. Jolicard, W. Karrlein, H. D. Meyer, N. Lipkin, O. Roncero, and R. Kosloff, *J. Comp.* **94**, 59 (1991).
38. Y. J. Yan and S. Mukamel, *J. Phys. Chem.* **93**, 6991 (1989); S. Mukamel and Y. J. Yan, *Acc. Chem. Res.* **22**, 301 (1989).
39. T. Joo, Y. Jia, J.-Y. Yu, D. M. Jonas, and G. R. Fleming, *J. Phys. Chem.* **100**, 2399 (1995).
40. R. Kumble, S. Palese, R. W. Visschers, P. L. Dutton, and R. M. Hochstrasser, *Chem. Phys. Lett.* **261**, 396 (1996).
41. R. W. Visschers, M. C. Chang, F. van Mourik, P. S. Parkes-Loach, B. A. Heller, P. A. Loach, and R. van Grondelle, *Biochemistry* **30**, 5734 (1991).
42. G. Doetsch, *Introduction to the Theory and Application of the Laplace Transformation*, Springer-Verlag, New York, Heidelberg, Berlin, 1974.